Dynamic Fracture Toughness Tests Of Dynamically Loaded Ductile Cast Iron

H.P. Winkler[1], R. Hüggenberg[1], A. Ludwig[2], G. Pusch[2], P. Trubitz[2],
[1] Gesellschaft für Nuklear-Service mbH, Essen, Germany;
[2] Technische Universität Bergakademie Freiberg, Freiberg, Germany
E-Mail: hans-peter.winkler@gns.de
E-Mail: ludwig@ww.tu-freiberg.de

1 Introduction

For a complete review of component safety, especially under accident conditions where as a result of rupture load conditions, rapid changes of stresses and deformations occur. For this characteristic dynamic fracture material values are necessary in order to calculate the stress conditions and to determine the margins against brittle fracture. The structure of Ductile Cast Iron (DCI) has a significant influence on the fracture toughness values. For the experimental determination of dynamic fracture toughness values, the existing guidelines deliver only initial approaches; they are orientated on the rule for static tests.

The paper describes an evaluation procedure that considers the influence of the structure on the behaviour of crack-propagation of Ductile Cast Iron at -40 °C regarding the experimental determination of dynamic R-curves, the definition of physical and technical crack initiation values and describes the influence of the graphite size, the correspondent ferrite grain size of the tensile properties and the fracture mechanic crack initiation values.

The assessment of the micro-structural-dependent crack resistance behaviour at room temperature and at -40 °C was done on static and dynamic crack resistance curves using the J-Integral concept. In the discussion it is shown that for the static case, the model of growing porosities and for the dynamic load case the micro cleavage fracture stress can describe the material behaviour.

2 Test Programme

The goal was to determine the dynamic fracture toughness characteristic values at -40 °C as a function of two different sample sizes and the microstructure. After casting three blocks, six sample blanks with the dimensions of length: 1360 mm, width: 150 mm, height: 290 mm, were machined from which large samples were prepared (thickness: 140 mm, width: 280 mm, length: 1350 mm), in the following referred to as SE(B)140 samples [1]. To avoid an anisotropic structure, the SE(B)140 sample blanks were manufactured by sand-casting under controlled conditions.
The small samples (thickness: 10 mm, width: 10 mm, length: 55 mm), in the following referred to as SE(B)10 samples, were prepared from the large samples in the region behind the fracture surfaces (Fig. 1).
The fatigue cracks were manufactured in accordance with the requirements of ASTM E 399-97 [2] and ESIS P2-92 [2].

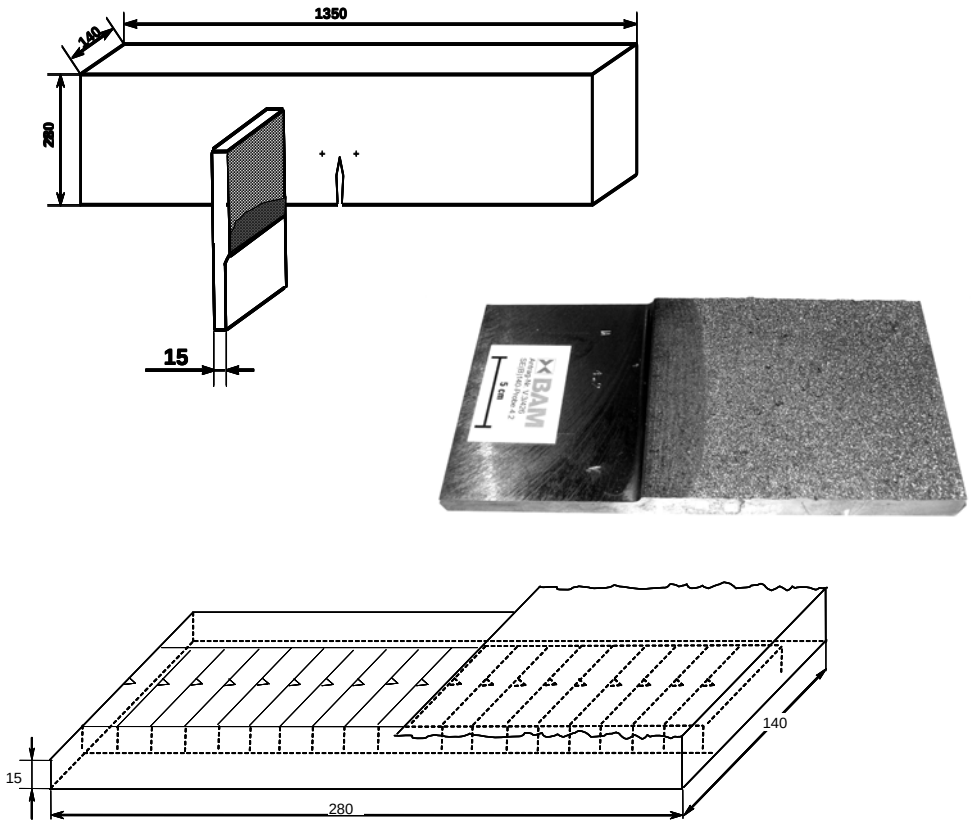

Fig. 1: Sample taking of the SE(B)10 samples (in mm)

3 Material

The examinations were performed on a ferritic Ductile Cast Iron (DCI) material containing globular graphite (Fig. 2).

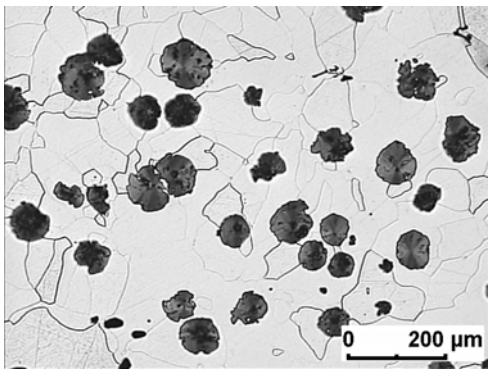

Microstructure parameters:

Diameter of the graphite nodules d_G	63 µm
Ferrite grain size d_F	62 µm
Particle distance λ	88 µm
Form factor f	0.71
Number of particles N_A:	47 mm^{-2}

Fig. 2: Typical microstructure of the test material

The mechanical properties are shown in Table 1.

Table 1: Mechanical characteristics at room temperature

$R_{p0.2}$ MPa	R_m MPa	A_5 %	Z %	E GPa	ν	HBW 2.5/187.5
246	362	11	13	172	0.28	138

4 Test methodology

4.1 Large samples

The loading of the SE(B)140 samples with fatigue cracking was carried out at -40 °C with the aid of a pulse testing machine with a loading rate of $5 \cdot 10^4$ MPa$\sqrt{m}$ s^{-1}[1]. The test preparation, procedure and evaluation were based on ASTM E399-97 [2].

4.2 Small samples

The experimental determination of the dynamic cracking resistance curves of the J-integral concept (J_d-Δa curves) was carried out on the 20 % side-notched SE(B)10 and precracked samples with fatigue cracking according to the "low-blow" technique using an instrumented pendulum impact tester. In the process, 6 to 8 samples in the region $2{,}8 \cdot 10^4 \text{ MPa}\sqrt{\text{m}}\,\text{s}^{-1} \leq \dot{K} \leq 5{,}7 \cdot 10^4 \text{ MPa}\sqrt{\text{m}}\,\text{s}^{-1}$ were loaded, the J_d values were determined via the dynamic force-displacement diagrams and the Δa values were determined on the fracture surfaces of the samples. The test was prepared, performed and evaluated according to ESIS P2-92 [3]. However, care must be taken that no stable ductile crack propagation takes place. The results of the raster electron microscopic fracture surface-analysis in Fig. 3 show that the Δa values for the entire range of the J_d-Δa curve in the result constitute a stable cleavage crack propagation.

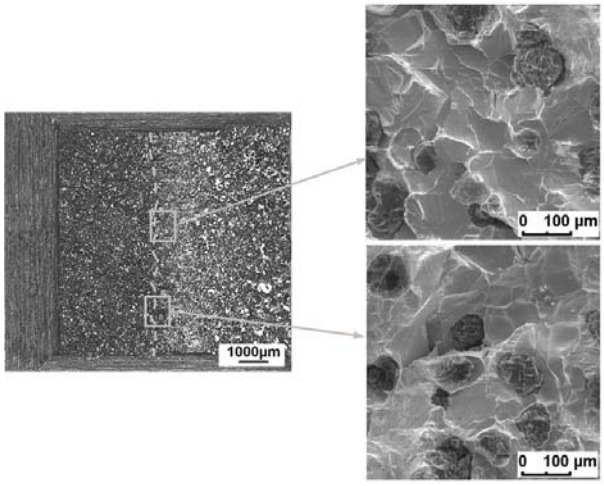

Fig. 3: Cleavage crack propagation on the fracture surface of the SE(B)10 samples at -40 °C

Thereby, it can be assumed that a global unstable crack propagation can be prevented by crack blunting (crack-tip-radius < graphite particle diameter) and energy-dissipative crack arresting (Fig.4).

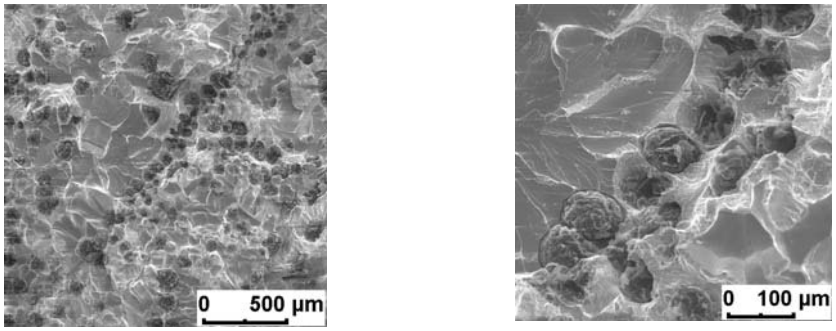

Fig. 4: Crack arresting at a graphite barrier

Since no stretch zone appears with this material-specific crack propagation, the definition of physical crack initiation values according to [3] in analogy to static loading is not possible. The applied procedure for recording and evaluating dynamic crack resistance curves of ferritic Ductile Cast Iron materials can be described as follows (Fig. 5):

1. Calculation and determination of the data points J_d and Δa according to ESIS P2-92

2. Determination of the dynamic crack initiation value $J_{di/\Delta a=0}$ at $\Delta a = 0$ mm at the intersection of the linearly extrapolated $J_{d\text{-}\Delta a}$ values by using the data in the range 0.1 mm $\leq \Delta a \leq$ 0.5 mm. In accordance with [3] $\Delta a_{max} = 0.5$ mm results of $\Delta a_{max} \leq 0.1$ (W-a) with W = sample width and a = crack length.

3. Determination of a dynamic crack initiation value $J_{d0,2}$. according to $\Delta a = 0.2$ mm.

4. Conversion of the J_d values to $K_{Id(J)}$ values according to $K_{Id}(J) = \left[\frac{J_d \cdot E}{1-\nu^2}\right]^{1/2}$ (1)

Fig. 5 shows furthermore that any processes damaging the microstructure, such as detachment of the graphite particles from the ferritic matrix or crack propagation between the particles, have an order of magnitude corresponding to the respective microstructural parameter.

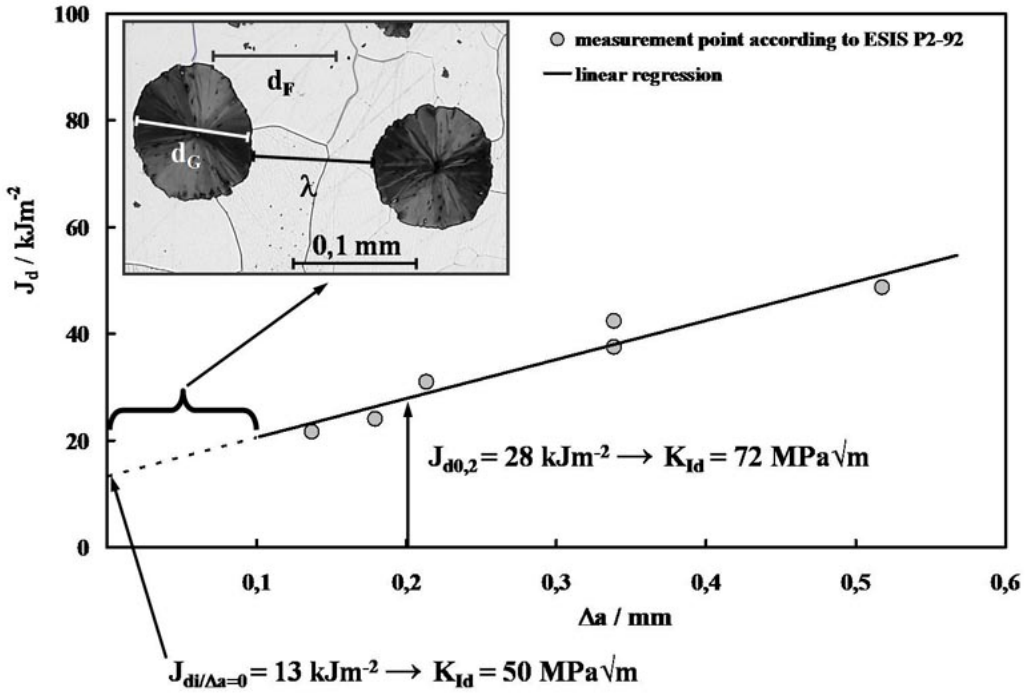

Fig. 5: J_d-Δa curve at -40 °C and definition of the dynamic crack initiation values

The dynamic fracture toughness values of the K and J integral concept determined with the small and large samples and the conversion according to equation (1) are shown in Table 2. Gray marked data are measured values, the other data are the converted values from measured data by using eq. (1).

Table 2: Dynamic fracture toughness values at -40 °C

Sample No.	SE(B)140 samples		SE(B)10 samples			
	K_{Id} MPa $\sqrt{m}$	$J_d(K_{Id})$ kJm^{-2}	$J_{di/\Delta a=0}$ kJm^{-2}	K_{Id} ($J_{di/\Delta a=0}$) MPa $\sqrt{m}$	$J_{d0,2}$ kJm^{-2}	K_{Id} ($J_{d0,2}$) MPa $\sqrt{m}$
1	67	24	13	50	28	72
2	71	27	17	56	31	76
3	75	30	16	56	37	83
4	79	33	17	56	32	77
5	71	27	19	59	27	71
6	64	22	24	66	34	79

The dynamic 0.2 % elongation limit was determined according to BS 7448-3 [4] via the corresponding strain rate at -40 °C with $R_{dp0.2} = 378$ MPa. Therewith, the K_{Id} values determined with the SE(B)140 samples fulfil the thickness criterion $B \geq 2{,}5\left(\frac{K_{Id}}{R_{dp0,2}}\right)^2$ (2)

and thus can be transferred to the component.

The scatter of the K_{Id} values in the range from $64\,\mathrm{MPa}\sqrt{m}$ to $79\,\mathrm{MPa}\sqrt{m}$ in a material-specific way and can be explained by the heterogeneity of the casting microstructure. This also applies for the dynamic toughness parameter values determined for the SE(B)10 samples with characteristic J_d-Δa curves according to Fig. 5.
The influence of the microstructure here becomes evident via the averaged random sampling of the six J_d-Δa curves (Fig. 6). The figure shows all single data-points of all small samples prepared from the large samples 1 to 6 (see Fig. 1).

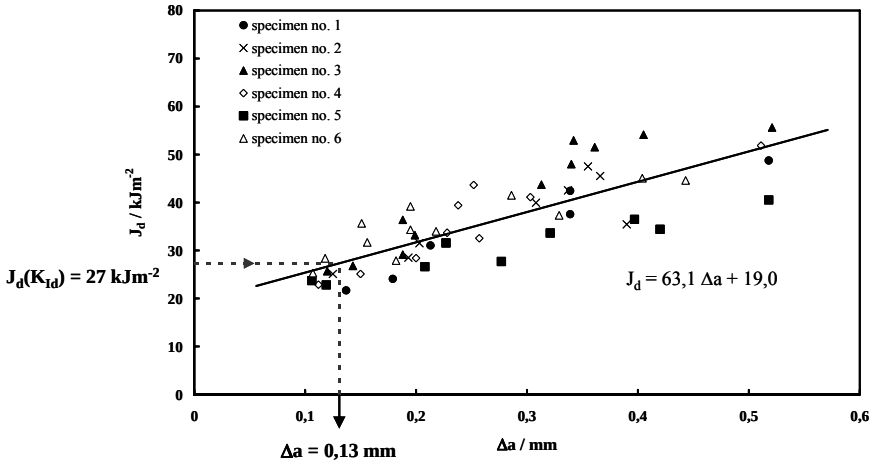

Fig. 6: Classification of the average value $J_{d(KId)}$ of the SE(B)140 samples in the averaged random sample of the J_d-Δa curve of the SE(B)10 samples (-40 °C)

For the average value of the SE(B)140 samples of $K_{Id} = 71 MPa\sqrt{m}$ or $J_{d(KId)} = 27\ kJm^{-2}$ follows for classification in the averaged random sample of the J_d-Δa curves a corresponding stable crack propagation for $\Delta a = 0.13$ mm (Fig. 11). This explains the large extent of agreement of the $J_{d(KId)}$ values or the K_{Id} values of the SE(B)140 sample with the $J_{d0.2}$ and $K_{Id(Jd0.2)}$ values determined according to ESIS P2-92 at $\Delta a = 0.2$ mm. The dynamic crack initiation values at $\Delta a = 0$ mm determined outside of ESIS P2-92 are more conservative, as expected.

5 Microstructural influence of the static and dynamic crack initiation values of ferritic cast iron Materials

The tests were performed in the same programme on DCI with a perlite content of ≤ 5 % with globular graphite nodules (Fig. 7).

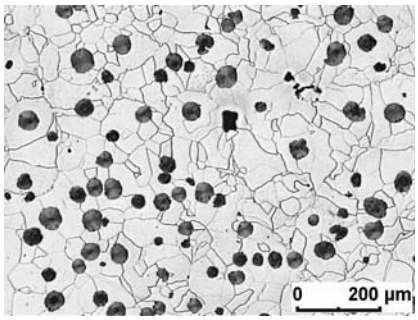

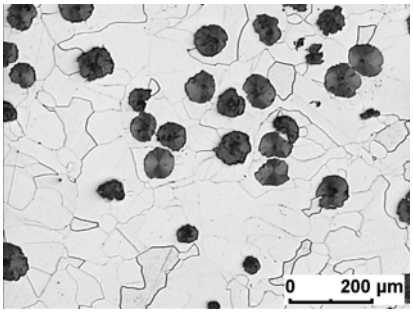

Fig. 7: Microstructure a) GJS (38), b) GJS (62)

The size of the ferrite grains and graphite nodules was varied as shown in Tab. 3. In accordance with the ferrite grain size, the materials are named as GJS (38) and GJS (62). The cast ingot was cooled on one side by a chill plate (d_G 38 µm) and on the other side by sand (d_G 62µm).

Table 3: Microstructure parameters of the graphite

DCI	V_G %	S_V 1/mm	N_A 1/mm²	d_G µm	d_F µm	f -	λ µm
GJS (38)	12	20	136	38	45	0.73	56
GJS (62)	15	12	48	62	63	0.71	86

V_G Volume of graphite
S_v Specific interphase graphite Ferrite
N_A Number of particles
λ Particle distance
d_G Diameter of the graphite nodules
d_F Ferrite grain size
f Form factor

5.1 Static Behaviour

The static fracture toughness values were determined as written in section 4.2. The crack resistance curves for both materials are shown in Fig. 8. It is clearly shown that the crack resistance of GJS (62) is higher than GJS (38). It can be concluded, that the crack resistance increases with growing the size of ferrite grains (d_F), growing diameter of the graphite nodules (d_G) and growing particle distance (λ). This is a result of the Strain-based crack initiation. It should be remarked that DCI is a typical model-material for particle-induced ductile fracture (Fig. 9), in which the distance of the particles has a significant influence on the initiation of crack propagation.

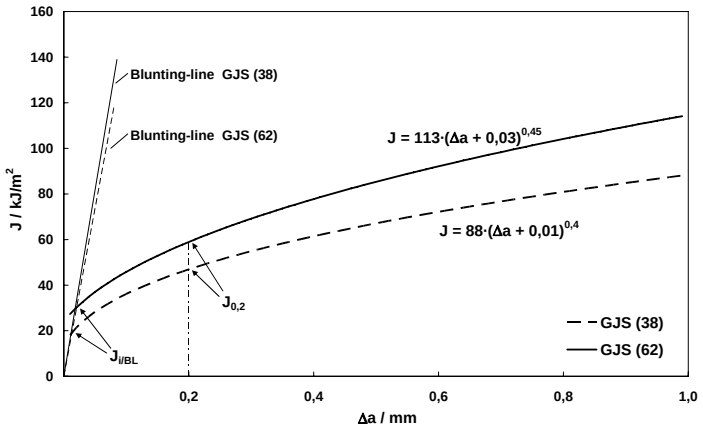

Fig. 8: Crack resistance curves for static test conditions (-40 °C)

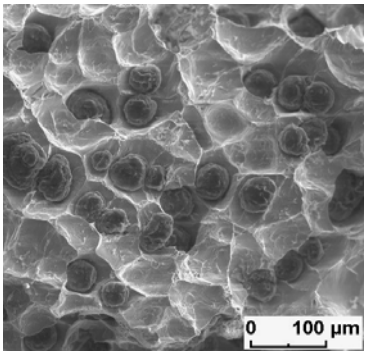

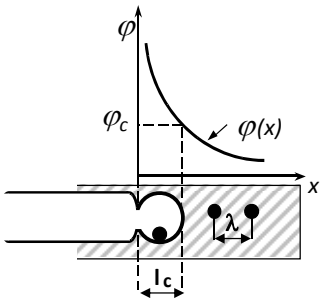

a) b)

Fig. 9: Strain-based crack initiation
a) SEM-Picture of the fracture surface of ferritic cast iron; b) Model

Therefore, a proportionality of the fracture toughness behaviour depending on the microstructure for static conditions is given such as that shown in Fig. 10.

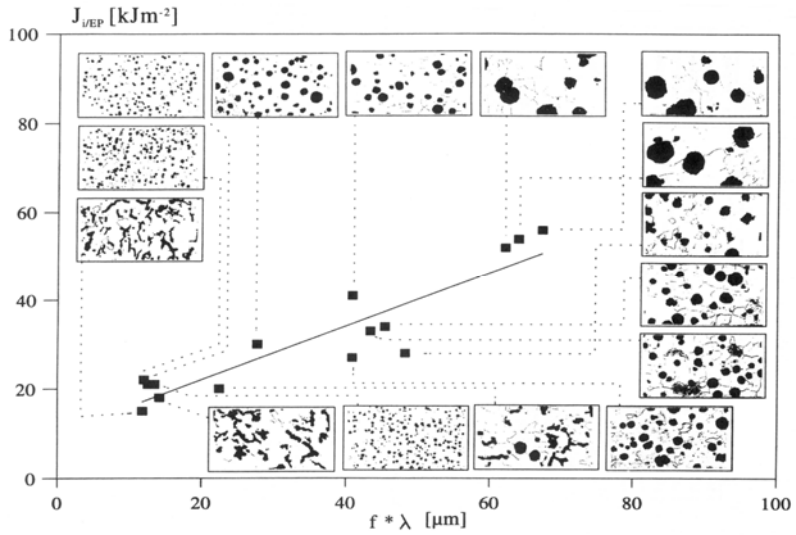

Fig. 10: Dependency of fracture toughness on microstructure of DCI for static conditions

5.2 Dynamic Behaviour

As shown in Section 4 in the case of a dynamic load, the micro-cleavage fracture stress is dominant. As an example, Fig. 11 shows the influence of different ferrite grain size (d_F), diameter of the graphite nodules (d_G) and Particle distance (λ). It can be concluded that the crack resistance decreases with growing the size of ferrite grains (d_F), growing diameter of the graphite nodules (d_G) and growing Particle distance (λ).

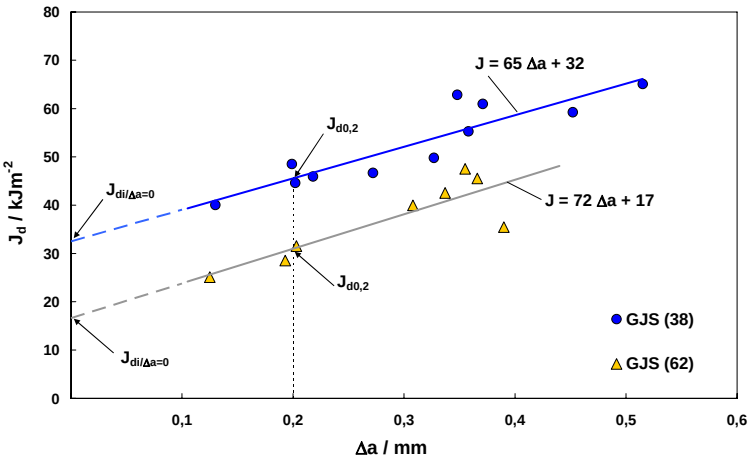

Fig. 11: Dynamic crack resistance curves (-40 °C)

6 Prospects for the future

Methods for the experimental determination of dynamic fracture toughness values on small specimens via recording of dynamic crack resistance curves can be realised using existing standards, [3], [5] or standard drafts [6]. The observed stable cleavage crack extension of ferritic Ductile Cast Iron material demands alternative definitions of physical crack initiation values. Finally this procedure is going to be published as a guideline of VDG (Association of German Foundry Experts). Further investigations are focussed on the transferability of these specific values to samples and components of differing thickness.

References

[1] W. Baer, Statistische Auswertung dynamischer Bruchmechanikversuche an Großproben aus ferritischem Gusseisen mit Kugelgraphit, 39. Tagung des DVM-Arbeitskreises Bruchvorgänge, Dresden, 13.-14.02.2007, Tagungsband, 319-328

[2] ASTM E 399-97, Standard Test Method for Plane-Strain Toughness of Metallic Materials, ASTM, 1997

[3] ESIS P2-92, Procedure for determining the fracture behaviour of metallic materials, European Structural Integrity Society, Delft, 1992

[4] BS 7448-3, Fracture mechanics toughness tests, Part 3: Method for determination of fracture toughness of metallic materials at rates of increase in stress intensity fracture greater than 3 MPam 0.5s-1, March 2003

[5] ISO 12135: Metallic materials – Unified method of test for the determination of quasistatic fracture toughness, December 2002

[6] ESIS TC5(2006), Proposed standard methods for instrumented pre-cracked Charpy impact testing of steel, Draft 26, March 2006. (Eingereicht bei ISO)